Physics of Sun and Star Spots
Proceedings IAU Symposium No. 273, 2010
A. C. Editor, B. D. Editor & C. E. Editor, eds.

doi:10.1017/S1743921311015870

Pre-Eruption Magnetic Configurations in the Active-Region Solar Photosphere

Manolis K. Georgoulis

Research Center for Astronomy and Applied Mathematics (RCAAM),
Academy of Athens, 4 Soranou Efesiou Street, Athens, Greece, GR-11527
email: manolis.georgoulis@academyofathens.gr

Abstract. Most solar eruptions occur above strong photospheric magnetic polarity inversion lines (PILs). What overlays a PIL is unknown, however, and this has led to a debate over the existence of sheared magnetic arcades vs. helical magnetic flux ropes. We argue that this debate may be of little meaning: numerous small-scale magnetic reconnections, constantly triggered in the PIL area, can lead to effective transformation of mutual to self magnetic helicity (i.e. twist and writhe) that, ultimately, may force the magnetic structure above PILs to erupt to be relieved from its excess helicity. This is preliminary report of work currently in progress.

Keywords. Sun: coronal mass ejections (CMEs), Sun: flares, Sun: magnetic fields

1. Introduction

Solar eruptions, that is, *solar flares* and *coronal mass ejections* (CMEs) are enigmatic dynamical manifestations in the solar magnetized atmosphere. The two phenomena do not always occur in pairs: not all flares are eruptive, that is, associated to CMEs, as much as not all CMEs are flare-associated (Yashiro *et al.*, 2004; Wang & Zhang 2007).

In solar active regions (ARs) there are mainly two types of eruptive photospheric magnetic configurations: cases of intense magnetic flux emergence/cancellation and cases of intense magnetic polarity inversion lines (PILs; see Forbes *et al.* [2006] for a review). Both involve intense photospheric flows: flux emergence is accompanied by flows carried from the sub-photosphere while PILs invariably exhibit strong shear flows. Often, one sees a combined situation with eruptions occurring above strong, *developing* PILs where flux persistently accumulates. In the quiet Sun, eruptions (CMEs) typically occur above extended, but weaker, PILs almost invariably outlined by unstable filaments in the low corona. Thus PILs are a prerequisite of most solar eruptions. For ARs, the development of strong PILs is long-known to lead to *at least* one *eruptive* flare before the PIL fades and the AR disappears from the disk (e.g. Hagyard *et al.* 1984). This is not the case with intense flux emergence that may or may not lead to eruptions.

Our inability to measure the coronal magnetic field has led to a debate over what magnetic structure(s) above PILs can actually trigger eruptions. The most obvious such structure is a *sheared magnetic arcade*, stretched due to the (observed) photospheric shear flows. Subject to strong shear and suitable topological conditions higher in the corona a sheared arcade may give rise to a *breakout* eruption (Antiochos *et al.* 1999). Another candidate structure is a *helical flux rope* (Rust & Kumar 1996) that is either emerged from the sub-photosphere or is formed prior to the eruption. A flux rope can give rise to more than one eruption scenarios (Forbes *et al.* 2006). A defining characteristic of flux ropes is their *magnetic helicity* (i.e., their internal twist and writhe) that, in some cases (helical kink instability) is the main driving force of eruptions. On the contrary, sheared arcades do not need helicity to trigger eruptions (Phillips *et al.* 2005).

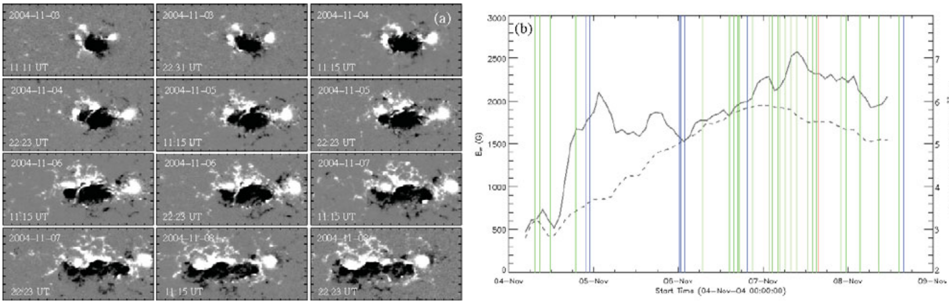

Figure 1. PIL evolution by magnetic flux accumulation and eruptive activity in NOAA AR 10696 over a 5-day period in 2004 November. (a) Timeseries of the photospheric magnetic configurations extracted from full-disk SoHO/MDI data. Tic mark separation in all images is 10″ (adapted by Georgoulis 2008). (b) Respective timeseries of the B_{eff}-values (left ordinate; solid curve) and the unsigned magnetic flux (right ordinate; dashed curve) in the AR. The vertical lines indicate the onset times of several flares, many of which were eruptive.C-, M-, and X-class flares are indicated by green, blue, and red, respectively.

2. Increasing PIL strength and implications

Why do strong PILs *always* host major eruptions? The free magnetic energy, consistently built-up due to electric currents as the PIL evolves but also consistently dissipated in small-scale, local reconnection episodes (EUV and soft X-ray "flickering") may not be the sole physical reason forcing strong PILs to always erupt. We argue that this is achieved by the coupling of free magnetic energy and *magnetic helicity*. This is *not* the same as claiming that a helical flux rope always pre-exists an eruption. Total helicity is roughly conserved in case of magnetic reconnection (e.g., Berger 1999). Free magnetic energy, on the other hand, cannot be totally released in the presence of helicity: theoretically, it can reach a minimum corresponding to a linear force-free magnetic structure with the prescribed helicity (Taylor 1974). The only option for the structure to relax is to bodily expel its excess helicity; this is a proposed CME mechanism (Low 1994). But how does helicity accumulate in the PIL area even if a flux rope is not physically present?

Aiming to quantify the PIL strength, Georgoulis & Rust (2007) introduced the *effective connected magnetic field strength* (B_{eff}), a measure of the magnetic connectivity in an AR. If $\Phi_{i,j}$ and $\mathcal{L}_{i,j}$ are the flux and length, respectively, connectivity matrix elements between the i ($i = 1, ..., p$) positive-polarity and the j ($j = 1, ..., n$) negative-polarity photospheric flux partitions, then $B_{eff} = \sum_{i=1}^{p} \sum_{j=1}^{n} (\Phi_{i,j}/\mathcal{L}_{i,j}^2)$. Clearly, large B_{eff}-values favor short connections in the AR. Developing PILs give rise to larger B_{eff}-values, tale-telling of eruptive ARs. In Figure 1 we show an example of the developing PIL in NOAA AR 10696 with the respective increase of B_{eff} and a resulting series of intensifying eruptive activity in the AR.

But does increasing B_{eff} imply increasing helicity even without a flux rope? This is possible, indeed: Georgoulis & LaBonte (2007) expressed the relative magnetic helicity H_m of an AR in the linear force-free approximation as $H_m = 8\pi \mathcal{F}_\ell d^2 \alpha E_p$, where d is the size element, α is the (constant) force-free parameter, E_p is the minimum (current-free) magnetic energy, and $\mathcal{F}_\ell$ is a known dimensionless parameter. If we now assume that there is a *single* magnetic flux tube with flux content Φ one can show that $\mathcal{F}_\ell E_p \simeq A\Phi^{2\delta}$ (details included in Georgoulis (2010)), where A is a constant and δ is a scaling index, with $1 < \delta \leqslant 1.2$. Then, magnetic helicity H_m can be written as $H_m = 8\pi d^2 \alpha A \Phi^{2\delta}$.

Now recall that H_m in an isolated flux tube reflects its twist T and writhe W, thus $H_m \sim (T + W)\Phi^2$ (Moffatt & Ricca 1992). Combining this and the above expression for

https://doi.org/10.1017/S1743921311015870 Published online by Cambridge University Press

H_m we can solve for the ratio $K \sim (W/T)$ between writhe and twist as follows:

$$K = \lambda \frac{W}{T} = \frac{8\pi d^2}{L} A \Phi^{2(\delta-1)} - \lambda \ . \tag{2.1}$$

Notice that K does *not* depend on the force-free parameter α. Instead, one needs the flux Φ, the footpoint separation L, and the geometrical parameter λ that reflects the coronal shape of the flux tube axis and connects T, L, and α via the equation $T = \lambda(\alpha L)$, assuming a thin coronal tube (Longcope & Klapper 1997). Georgoulis (2010) determines the extremes of λ: $\lambda \in [1/(4\pi), 1/8]$, from a highly eccentric elliptical flux tube to a semi-circular flux tube. For a single flux tube $B_{eff} = \Phi/L^2$, so Eq. (2.1) gives

$$K = \frac{8\pi d^2}{L^{5-4\delta}} A B_{eff}^{2(\delta-1)} - \lambda \ . \tag{2.2}$$

Therefore, large B_{eff}-values, hence intense PILs, favor $K > 0$. However, $K > 0$ means that the twist and writhe have the same sign, which is a *necessary* condition for the helical kink instability (Rust & LaBonte 2005).

3. Discussion and Conclusion

We showed that increasing PIL strength, via persistent flux accumulation along it, implies directly an increasing likelihood of triggering of the helical kink instability in the PIL, at least in case of a single flux tube.

The fundamental requirement of the helical kink instability, however, is the existence of strong twist (self-helicity) that is not evident in case of a sheared arcade. Instead, a sheared arcade includes substantial mutual helicity (Régnier *et al.*, 2005; Démoulin *et al.* 2006). There is only one way to transform mutual into self helicity and this is via magnetic reconnection that roughly conserves the total helicity. Notice from Eq. (2.1) how the kink instability with large writhe favors short footpoint distances ($K \propto 1/L$) in the unstable flux tubes which aligns with the small-scale nature of magnetic reconnection.

We argue, and show in Georgoulis (2010), that the small-scale flickering of numerous magnetic reconnection events always observed in PILs effectively transforms large amounts of the shear-induced mutual helicity into self helicity. Small-scale kinks form and reconnect with the overlying structure (the sheared arcade), transferring their self-helicity to it. The larger structure evolves through increasingly unstable states and finally erupts to shed its excess helicity. The eruption can happen when overlaying conditions are suitable (i.e. minimal confinement), when the overall twist exceeds the kink-instability threshold (large-scale kink), or when a locally initiated sequence of magnetic reconnections causes such intense energy dissipation that the system cannot stay confined.

Notice how this general scenario (1) encompasses flux cancellation models, refining them with a resulting inverse cascade of magnetic helicity from smaller to larger scales, (2) does not remand a pre-existing flux rope, but may allow its formation prior to eruption, and (3) explains the necessity of strong PILs to always erupt.

Figure 2 shows an illustrative example of calculating $K + \lambda$ via Eq. (2.1). A series of roughly coaligned soft X-ray images of the AR are also provided (Figures 2a-c). Notice that candidate locations for the small-scale helical kink instability are *exclusively* along the flux-massive PIL. When the number and cumulative flux of these candidate locations maximized - creating maximum-likelihood conditions for the helical kink instability - a major eruption associated with a X2.3 flare was triggered in the AR. The eruption started locally, from a magnetic structure precisely within the candidate unstable locations and resembled an unstable kink in X-rays (Figure 2c).

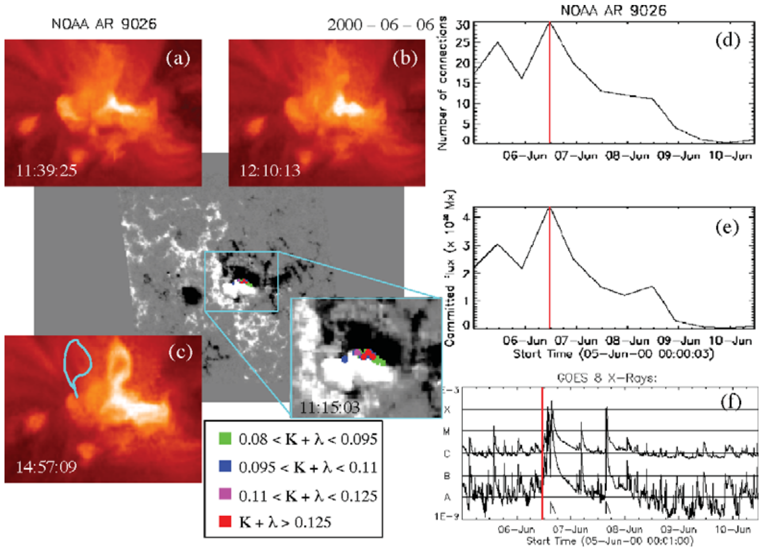

Figure 2. Calculation of candidate kink-unstable connections in NOAA AR 9026 on 2000 June 6. The small-scale connections satisfying $K > 0$ are shown in different colors; from green (weakest; $\lambda \simeq 0.08$) to red (strongest; $\lambda \simeq 0.125$). The X-ray images of the AR (a-c) sample pre-eruption instances. An apparently small-scale kink-unstable structure initiated the eruption (c); a hand-drawn cyan curve next to the loop exemplifies its shape. On the right, the plots show the number of candidate kink-unstable locations (d), their cumulative flux (e), and the GOES X-ray plot (f). The red vertical line in these plots indicates the magnetogram time (11:15 UT).

Acknowledgements

I gratefully acknowledge financial support by the Organizers to attend the Symposium.

References

Antiochos, S. K., DeVore, C. R., & Klimchuk, J. A. 1999, *ApJ*, 510, 485
Berger, M. A., 1999, *Plasma Phys. Contr. Fusion*, 41, B167
Démoulin, P., Pariat, E., & Berger, M. A. 2006, *Solar Phys.*, 233, 3
Forbes, T. G., *et al.* 2006, *Space Sci. Revs*, 123, 251
Georgoulis, M. K. 2008, *Geophys. Res. Lett.*, 35, L06S02, doi:10.1029/2007GL032040
Georgoulis, M. K. 2010, *Solar Phys.*, in preparation
Georgoulis, M. K. & LaBonte, B. J. 2007, *ApJ*, 671, 1034
Georgoulis, M. K. & Rust, D. M. 2007, *ApJ*, 661, L109
Hagyard, M. J., Teuber, D., West, E. A., & Smith, J. B. 1984, *Solar Phys.*, 91, 115
Longcope, D. W. & Klapper, I. 1997, *ApJ*, 488, 443
Low, B. C. 1994, *Phys. Plasmas*, 5, 1684
Moffatt, H. K. & Ricca, R. L. 1992, *Proc. Math. Phys. Sci.*, 439, 411
Phillips, A. D., Macneice, P. J., & Antiochos, S. K. 2005, *ApJ*, 624, L129
Régnier, S., Amari, T., & Canfield, R. C. 2005, *A&A*, 442, 345
Rust, D. M. & Kumar, A. 1996, *ApJ*, 464, L199
Rust, D. M. & LaBonte, B. J. 2005, *ApJ*, 622, L69
Taylor, J. B. 1974, *Phys. Rev. Lett.*, 19, 1139
Wang, Y. & Zhang, J. 2007, *ApJ*, 665, 1428
Yashiro, S., Gopalswamy, N., Michalek, G., St. Cyr, O. C., Plunkett, S. P., Rich, N. B., & Howard, R. A. 2004, *J. Geophys. Res.*, 109(A7), A07105

Discussion

NAME: DIALOG